

Dielectric Relaxation of Water Absorbed in Porous Glass

Ya. Ryabov,^{†,‡} A. Gutina,[†] V. Arkhipov,^{†,§} and Yu. Feldman^{*,†}

Department of Applied Physics, The Hebrew University of Jerusalem, Givat Ram 91904, Jerusalem, Israel, Institute of Mechanics and Engineering of Kazan Scientific Center of Russian Academy of Sciences, Lobachevsky st. 2/31, Box 559, 420111, Kazan, Russia, and The Kazan State University, Kremlevskaya st. 18, 420008, Kazan, Russia

Received: September 16, 2000; In Final Form: December 11, 2000

The dielectric spectroscopy method was applied to the investigation of water absorbed on the inner surface of porous glass. The measurements were done using broad band dielectric spectrometry (BBDS) over a wide range of frequency (20 Hz to 1 MHz) and temperature (−100 °C to +300 °C). The dielectric response was found to be very sensitive to the geometrical micro- and mesostructural features of the porous matrix and the structure and mobility of the water filling the pores. The hindered dynamics of water molecules located within the pores and affected by the surfaces reflect the geometrical structure of the porous matrix. The analysis of the dielectric parameters as a function of the temperature enabled us to characterize the physical parameters of the dielectric spectra over an extended frequency range.

1. Introduction

Recently, much attention has been paid to the properties of water adsorbed to surfaces of porous silica glasses.^{1,2} These glasses can be defined as random structures of two interpenetrating, percolating phases—the solid and the pore networks. The pores in the glasses are connected to each other, and the pore size distribution is narrow. The characteristic pore spacing depends on the method of preparation and can range between 2 and 500 nm.³

It has been shown⁴ that silica glasses contain three types of adsorbed water on the pore surface. The first type forms a physisorbed layer. The second type forms a chemisorbed layer associated with spatially distributed individual molecules (or groups of several molecules) on the surface. The third type is a more strongly chemisorbed layer. It consists of water clusters of 40–60 molecules⁴ connected to each other by hydrogen bonds and forming an ordered array of water molecules.

The dynamic properties of the absorbed water, obtained from NMR and dielectric spectroscopy, are different from those of the bulk water due to the geometrical confinement of the liquid in the pores and interaction of the molecules with active surface sites.^{5,6}

In our previous paper,⁷ we studied the dielectric properties of silica glasses over broad frequency and temperature ranges in order to investigate the dynamics and the morphological properties of the porous materials. It was shown that the complex dielectric behavior could be described in terms of four distributed relaxation processes. The typical spectrum of the dielectric losses associated with a relaxation of water molecules in the absorptive layer of the studied porous glasses versus frequency and temperature is displayed in Figure 1.

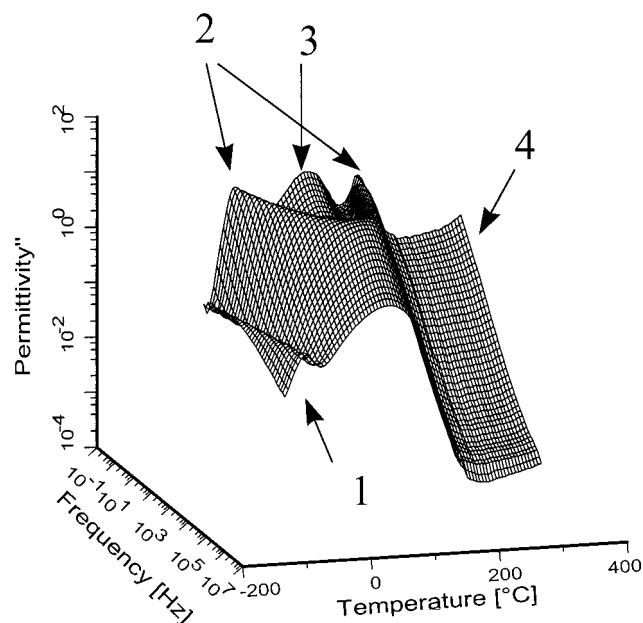


Figure 1. Three-dimensional plot of the characteristic frequency and temperature dependence of the dielectric losses for the porous glass (Reproduced from ref 7. Copyright 1998, Elsevier Science).

The first relaxation process, which is observed in the low-temperature region from −100 °C to +10 °C, is due to the reorientation of water molecules in ice-like water cluster structures. The hindered dynamics of the water molecules located within the pores reflect the interaction of the absorptive layer with the inner surfaces of the porous matrix.

The second relaxation process has a specific saddle-like shape and is well marked in the temperature range of −50 °C to +150 °C. This relaxation process is thought to be a kinetic transition due to water molecule reorientation in the vicinity of a defect.

The third process is located in the low-frequency region and the temperature interval 50 °C to 80 °C. The amplitude of this process essentially decreases when the frequency increases and the maximum of dielectric losses has almost no temperature

* Author to whom correspondence should be addressed at School of Applied Science, The Hebrew University of Jerusalem, Givat Ram, 91904, Jerusalem, Israel. Tel: +972 2 6586187. Fax: +972 2 5663878. E-mail: yurif@vms.huji.ac.il.

[†] The Hebrew University of Jerusalem.

[‡] Institute of Mechanics and Engineering of Kazan Scientific Center of Russian Academy of Sciences.

[§] The Kazan State University.

TABLE 1: The Pore Size, Porosity, and Humidity of the Samples

samples	pore size, nm	porosity Φ , %	humidity, %
A	50–70	38	1.2
B	50–70	48	1.4
C	280–400	38	3.2

dependence. This relaxation process is related to the percolation of dipole moment excitation within the developed fractal network structure of connected pores due to the self-diffusion of the charge carriers filling the porous space. Note that the fractality mentioned here is related to the fractal dimensions of the transfer paths connecting the hydration centers located on the inner surface of the pores.⁸

The fourth process. In the high-temperature region, above 150 °C, the glasses become remarkably electrically conductive and show an increase in dielectric constant and dielectric losses in the low-frequency limit. This relaxation process is thought to be related to the Maxwell–Wagner–Sillars polarization process as a result of the trapping of free charge carriers at the interface, thus causing buildup of macroscopic charge separation or space charge with a relatively long relaxation time.

In this paper we will discuss in detail the first and the second relaxation processes.

2. Experimental Section

Sample Preparation. Three different porous silica glasses, labeled A, B, C, were fabricated by the leaching of sodium borosilicate glass with phase separation in an acid solution, according to methodology described elsewhere.^{3,9} The initial glass was subjected to heat treatment at 490 °C for 165 h (glass A) and 650 °C for 100 h (glass C). All samples were then etched in hydrochloric acid and rinsed in deionized water. Glass B was obtained from glass A by additional immersion in KOH solution. This sample was also rinsed in deionized water. The resulting glasses have different structures. It is known from the technology of sample fabrication that sample A contains silica gel in the pore's volume. However, the silica gel is barely present in the other samples.

The porosity of all the samples was determined by the relative mass decrement method. The dimensions of the pores were calculated from absorption–desorption isotherms and from electron microscope photographs of the porous samples.³ The magnitudes of the pore sizes obtained from these two methods concur. However, if the pores are filled up with silica gel, then neither of these methods is accurate for determining the pore sizes. The relative water content to the dry sample was determined by weighing the samples prior to and immediately after the dielectric measurements. The dimensions of the pores, porosity, and humidity of the samples are presented in Table 1.

Experimental Technique. Dielectric measurements in the frequency range of 20 Hz–1 MHz were performed by using a Broad Band Dielectric Spectrometer BDS 4284 (NOVOCONTROL) with automatic temperature control by QUATRO Cryosystem. The accuracy of the complex dielectric permittivity measured ($\epsilon^*(\omega) = \epsilon'(\omega) - i\epsilon''(\omega)$, where $\epsilon'(\omega)$ and $\epsilon''(\omega)$ are the real and loss parts of the complex permittivity, respectively) was estimated to be better than 3%.¹⁰ The samples were measured at intervals of 5 °C upon heating them from –100 °C to 300 °C. The size and thickness of the square plate samples, used for dielectric measurements, were 30 mm and 0.31–0.32 mm, respectively.

For a quantitative analysis of the dielectric spectra for all the relaxation processes a superposition of the Havriliak–Negami

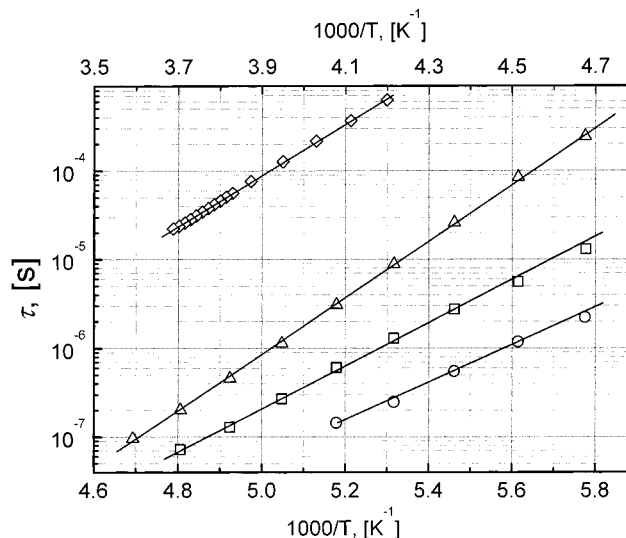


Figure 2. Temperature dependence of the characteristic relaxation time of the first process for samples A (squares), B (circles), C (triangles), and relaxation time of bulk ice (rhombuses). The top axis corresponds to the temperature behavior of bulk ice. The solid lines correspond to the Arrhenius fit. The activation energies $\Delta H_A = 50$ kJ/mol, $\Delta H_B = 42$ kJ/mol, $\Delta H_C = 67$ kJ/mol, $\Delta H_{ice} = 60$ kJ/mol. The small deviation in Activation Energies values between those presented in the paper⁷ (Figure 3) and in this figure are due to the more advanced way of data treatment used recently.

(HN) formula $\Delta\epsilon_j/[1+(i\omega\tau_j)^{\alpha_j}]^{\beta_j}$ and Jonscher's empirical term $(i\omega)^{n_j}$ has been fitted to the isothermal data of the complex dielectric permittivity.⁷ Here $\Delta\epsilon_j$ is the dielectric strength and τ_j is the mean relaxation time. The index j refers to the different processes, which contribute to the dielectric response. The parameters α_j and β_j describe the symmetric and asymmetric broadening of the relaxation process; n_j is a Jonscher parameter for the high-frequency part of the respective relaxation process. In the case of a relaxation process including a contribution of electrical conductivity, the additional conductivity term was applied.

3. Results and Discussion

The First Relaxation Process. The temperature dependencies of the relaxation times of the first process for the samples A, B, and C (see Figure 2) demonstrate Arrhenius behavior. The energies of activation ΔH of this process are dependent on the water content, the microstructure of the pore surface, and the amount of silica gel inside the pores. In the works^{6,11} a similar dielectric relaxation behavior in silica–water systems with low water content has been observed recently and ascribed to the reorientation of water molecules in ice-like structures. The formation of this ice-like water structure is strongly dependent on the amount of water covering the pore surface. The calculated value of the activation energy for sample C (ΔH_C) is in good agreement with the activation energy of bulk ice ~ 60 kJ/mol.¹² This fact can be explained by the following reason. In sample C there is enough water inside the pores for the formation of the ice-like structure. The higher activation energy for the porous glass sample C can be explained by the strong interaction of chemisorbed water molecules with the inner surface of the matrix. In the case of samples A and B, the activation energies are significantly smaller than ΔH_{ice} . This is most probably associated with the deficit of water molecules required for the construction of ice-like clusters. In the case of sample A, the water is confined in the very small pores of the silica gel. Thus,

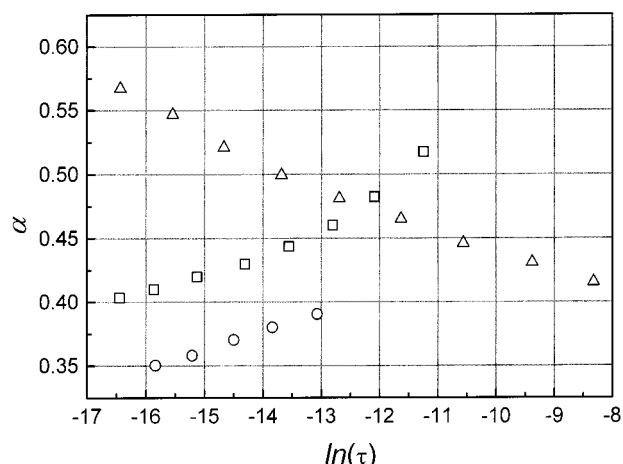


Figure 3. The dependence of the Cole–Cole α parameter on $\ln(\tau)$ for samples **A** (squares), **B** (circles), **C** (triangles).

we have a more rigid water structure than for the sample **B**, which is confirmed by the values of the activation energies of this process.

Unlike the Debye relaxation of bulk ice, the relaxation of all the samples markedly demonstrate the non-Debye Cole–Cole type behavior

$$\epsilon^*(\omega) = \epsilon_{\infty} + \frac{\epsilon_s - \epsilon_{\infty}}{1 + (i\omega\tau)^{\alpha}} \quad (1)$$

where τ is the mean relaxation time of the process, ω is the cyclic frequency, ϵ_s and ϵ_{∞} are the low- and high-frequency limits of dielectric permittivity, respectively, and α is the Cole–Cole parameter. It is known from the literature^{13,14} that the parameter α is strictly dependent on temperature, structure, composition, and other controlled physical parameters of the complex materials, while the relaxation time also depends on the same physical parameters of the sample. Thus, it is quite possible that parameters α and τ are naturally related to each other. In the work¹⁵ the experimental dependency of the Cole–Cole α parameter on relaxation time τ for the polymer–water mixtures was already reported. A correlation between $\alpha(\tau)$ behavior and the hydrophilic properties of polymer chains was found.

A similar $\alpha(\tau)$ behavior was observed in the case of the first relaxation process. Figure 3 represents the dependencies of the parameter α on the relaxation times for all the samples. Two different types of parameter α dependencies versus the relaxation time correlated strictly with the amount of absorbed water could be detected. The largest amount of water in sample **C** led to a decrease of parameter α with an increase of the relaxation time, while the smaller water amount in samples **A** and **B** tended to inverse the $\alpha(\tau)$ behavior (see Figure 3 and Table 1). The positive slopes of samples **A** and **B** could be explained by the significant number of water molecules directly interacted with the glass matrix. For sample **C**, with a negative slope of $\alpha(\tau)$ dependence, only a limited amount of water molecules still interacted with the glass surface.

Let us compare the dielectric strength of the first relaxation process with the amplitude of the dielectric relaxation of bulk ice. In this case we have to recalculate the dielectric permittivity of bulk ice to the equivalent volume of water absorbed in a unit volume of porous glass. This calculation can be performed using a simple mixture formula.¹⁶ For example, for sample **C**, taking into account the static dielectric permittivity of bulk ice $\epsilon_s \approx 100$, the dielectric permittivity of air $\epsilon_a = 1$, the dielectric

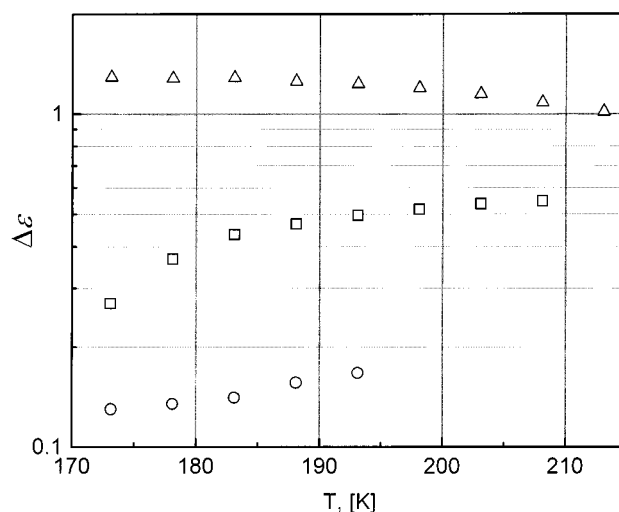


Figure 4. The temperature dependencies of the dielectric strength of the first relaxation process for samples **A** (squares), **B** (circles), **C** (triangles).

permittivity of glass matrix $\epsilon_{gm} = 3.2$ and the values of porosity and humidity from Table 1, one can obtain the effective dielectric strength of bulk ice $\Delta\epsilon_{ice}^{eff} = 3.5$. Thus the dielectric strength (see Figure 4) of the first relaxation process is significantly smaller than the dielectric strength of the bulk ice.¹⁷ There are two possible explanations for this difference: (a) not all the water molecules are participating in this process; (b) the structure of the water absorbed on the surface of porous glasses is different from that of water in the bulk ice and there is a tendency toward antiparallel orientation of the water molecules.

To clarify this issue let us discuss the character of dipole orientation correlations. We can do this using Fröhlich's approach:

$$\frac{\Delta\epsilon_1(2\Delta\epsilon_1 + 3\epsilon_{\infty})}{\Delta\epsilon_1 + \epsilon_{\infty}} T = \frac{4\pi n}{3k} \overline{mm^*} \equiv B(T) \quad (2)$$

where m^* represents the average dipole moment of a spherical region embedded in its own medium, if one of its units is kept in a given configuration leading to a dipole moment m , mm^* is the average value of the product mm^* taking into account all possible configurations and weighing them according to the probability of finding the unit in such a configuration.¹⁸ m^* is different from m due to the existence of short-range forces or due to the nonspherical shape of molecules. According to Fröhlich's theory monotonic growth of the function $B(T)$ with increasing temperature means the tendency toward antiparallel orientation of the relaxing dipole units. The monotonic decreasing of the function $B(T)$ with increasing temperature signifies the tendency toward parallel orientation, while the constant value of the function $B(T)$ with the change in temperature corresponds to a noncorrelated system. Figure 5 demonstrates the clear tendency toward the antiparallel orientation of the water dipoles for samples **A** and **B**. For sample **C**, the inclination toward the antiparallel orientation at low temperatures turns to a tendency toward parallel orientation at high temperatures.

It is known¹⁹ that for a bulk ice the water dipoles have a tendency to form parallel orientations due to the tetrahedral bulk structure. In our case, the water molecules in the interface cannot form this kind of structure and, therefore, they have a tendency to form antiparallel orientation. Thus, in this case the tendency toward the antiparallel orientation for samples **A** and **B** is due to the nondipole short-range interactions in two-dimensional

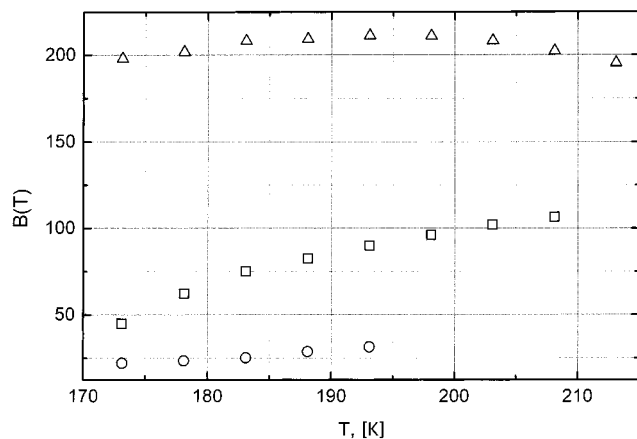


Figure 5. The temperature dependence of function $B(T)$ for samples **A** (squares), **B** (circles), **C** (triangles).

clusters. In contrast, for sample **C** there is a comparatively large amount of water and a small specific porous surface. In this case the nonmonotonic $B(T)$ behavior is a result of the competition between the surface and the bulk effects.

The qualitative measure of the dipole correlation rate is the Kirkwood correlation factor g . It is possible to estimate g directly by using the Kirkwood formula:¹⁸

$$\frac{\Delta\epsilon_1(3\epsilon_{s_1} - \Delta\epsilon_1)}{\epsilon_{s_1}} = \frac{4\pi\mu^2 gn}{kT} \quad (3)$$

where the dielectric strength $\Delta\epsilon_1 = \epsilon_{s_1} - \epsilon_{\infty_1}$ was evaluated from the fitting procedure (ϵ_{s_1} and ϵ_{∞_1} are the low- and the high-frequency limits of the dielectric permittivity of this process), μ is the value of the water molecule dipole moment in the liquid phase, k is the Boltzmann constant, and T is the absolute temperature. However, from eq 3 one can only evaluate the product gn , where n is the molar concentration of water molecules involved in the first relaxation process. Since samples **A** and **B** have a small water content and a well-developed porous surface, all the water molecules are situated in the interface and can participate in the first relaxation process. Therefore, we can estimate the molar concentration of water molecules n as the product of humidity h and Avogadro Number N_A : $n = N_A h$. Thus, for samples **A** and **B**, one obtains the Kirkwood correlation factor $g \ll 1$ ($g \in [0.02, 0.04]$ for the sample **A** and $g \in [0.008, 0.011]$ for sample **B**). For sample **C**, with a large water content and small pore surface, the water molecules are situated in the interface as well as in the bulk. Therefore, the water in sample **C** cannot be considered as a uniform structure and consequently cannot be treated by eq 3.

It has already been mentioned that the activation energy of the first relaxation process for all the samples is similar to the activation relaxation energy of bulk ice. However, the mean relaxation time for this process is much shorter than the one for bulk ice. This phenomenon has its origin in the relaxation process mechanism.

It is well-known that structure defects play a very important role in the dielectric relaxation of bulk ice. The long dielectric relaxation time in bulk ice ($\sim 10^{-5}$ s) can be explained as follows: a water molecule waits a relatively long time for a defect to migrate to its lattice site but when one arrives, it reorients very rapidly ($\sim 10^{-11}$ s).¹⁹ The water molecules situated at the water–air interface have no regular three-dimensional structural features. Therefore, the heat fluctuation is able to reorient these water molecules independently of the presence

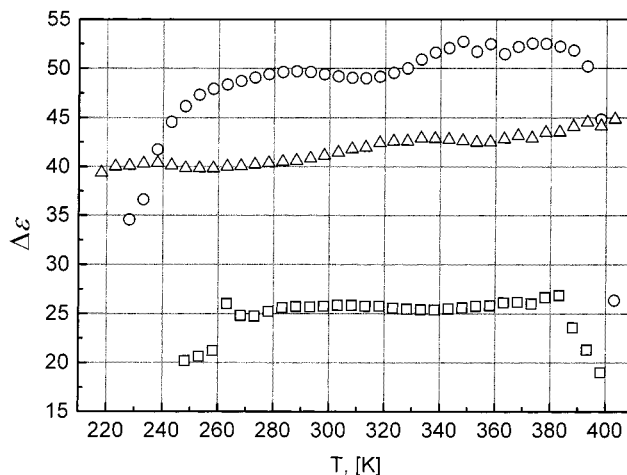


Figure 6. The temperature dependence of the dielectric strength of the second relaxation process for samples **A** (squares), **B** (circles), **C** (triangles).

of a defect in the vicinity. Thus, the first relaxation process is due to water molecule reorientation in the interface, which can occur any time. Therefore, the probability of reorientation in the bulk depends on the presence of a defect and is much smaller than the probability for reorientation in the interface. This explains why the relaxation time of the first process is shorter than that for the bulk ice, even though the same number of hydrogen bonds is breaking during the reorientation for both interface and bulk water molecules. This explains why the energies of activation for the first relaxation process and for bulk ice are similar.

Thus the mechanism of the first relaxation process is different from that of dielectric relaxation in bulk ice. It is independent of the defect concentration. Nevertheless, defect mobility is very important for relaxation of the water absorbed in porous glasses and will be discussed in connection to the second relaxation process.

The Second Relaxation Process. The relaxation process manifested in the temperature range -50 °C to $+150$ °C has a specific saddle-like shape (see Figure 1). The amplitude of this process remains approximately constant in the whole temperature range where this process occurs (see Figure 6). Thus, despite heating, the number of the relaxation units participating in the process practically does not change.

To describe the second relaxation process we developed a model based on the idea of Macedo and Litovitz.²⁰ This model considers the relaxation act as an occurrence of two simultaneous events: (a) the molecule must attain sufficient energy to break away from its neighbors and change its orientation, and (b) there must be a site with a defect in the vicinity of the moving molecule with sufficient local free volume for a reorientation to occur. The probability of a transition from one orientation of the molecule to another is given by

$$P = P_a P_d \quad (4)$$

where P_a is the probability of attaining sufficient energy to break the bonds and P_d is the probability that there is a defect, i.e., sufficient local empty space near the molecule for its reorientation to occur.

The probability P_a can be calculated on the basis of the activation theory of Eyring.²¹ In the simplified form it reads

$$P_a \cong \exp(-H_a/kT) \quad (5)$$

where H_a is the height of the potential barrier between equilibrium positions. On the other hand, the probability of defect formation P_d can be described within the free volume conception and estimated within the framework of the Cohen and Turnbull approach.²² According to this approach, P_d can be calculated as the probability of finding the volume V^* of a defect necessary for a molecule reorientation to occur and is given by

$$P_d \cong \exp(-V^*/V_f) \quad (6)$$

where V_f is the average free volume per defect. One should bear in mind that the value of the volume V^* is close to the value of the molecule volume. Hence, since $V^* \ll V_f$ the volume of water clusters in the system can be estimated as $V = (V^* + V_f)N \approx V_f N$, where N is the total number of the defects in the system. Thus, eq 6 can be rewritten as

$$P_d \cong \exp(-V^*N/V) \quad (7)$$

The free volume concept as it was introduced in ref 20 deals with a constant number of molecules and considers the temperature dependence of the free volume. In contrast, in the case of water absorbed in porous glasses the number of defects can depend on the temperature. We assume that the temperature dependence of the number of defects N can be described by Boltzmann's Law:

$$N = N_0 \exp\left(-\frac{H_d}{kT}\right) \quad (8)$$

where N_0 is the average number of water molecules in the cluster, and H_d is the energy of the defect formation. By substituting eq 8 into eq 7 and taking into account that the volume of the water clusters, V , varies with temperature as a linear function, i.e., far less than the exponential term, we obtain

$$P_d \cong \exp\left(-\frac{V^*N}{V}\right) = \exp\left(-C \exp\left(-\frac{H_d}{kT}\right)\right) \quad (9)$$

where $C = V^*N_0/V$. According to the definition, the ratio V/V^* is the maximum possible number of defects in the ice-like water cluster. Thus, there is a clear physical meaning for constant C :

$$C = \frac{1}{\eta} \quad (10)$$

where constant η is the maximum possible defect concentration.

Assuming that the relaxation time is inversely proportional to the transition probability and taking into account eqs 5 and 9, we obtain the equation

$$\tau = \tau_0 \exp\left\{\frac{H_a}{kT} + C \exp\left(-\frac{H_d}{kT}\right)\right\} \quad (11)$$

which describes the temperature dependence of the relaxation time corresponding to the second relaxation process of water absorbed in silica glasses. The preexponential constant τ_0 can vary with temperature, but far less than the exponential term.

The experimental data of the relaxation time were fitted to eq 11 by means of a least-squares procedure. The fitting curves are shown in Figure 7 (solid line). The fitting curves show a rather good agreement between the experimental temperature dependence of the mean dielectric relaxation time of the second process and the behavior obtained on the basis of the simple

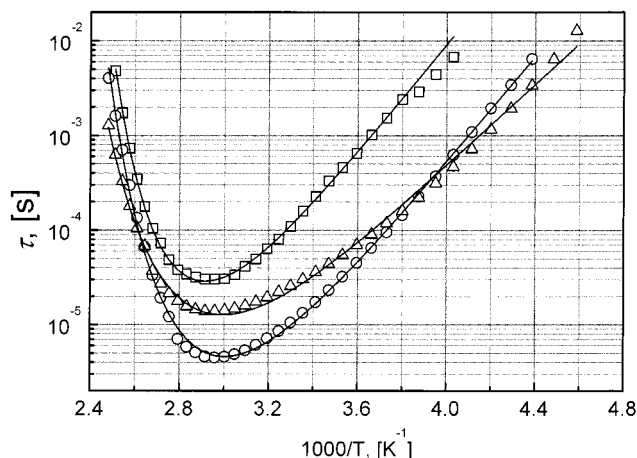


Figure 7. The temperature dependence of the relaxation time of the second relaxation process for the samples **A** (squares), **B** (circles), **C** (triangles). The solid lines correspond to the fit.

TABLE 2: The Result of the Fitting According to Equation 11

sample	H_a , kJ/mol	H_d , kJ/mol	τ_0 , s	η
A	55	39	3×10^{-14}	9×10^{-7}
B	54	31	3×10^{-15}	8×10^{-6}
C	42	30	9×10^{-13}	2×10^{-5}

model developed. The model can be applied to the interpretation of the dynamics of water molecules adsorbed by the active hydrate centers and forming water clusters distributed on the pore surface.

According to the mechanism suggested in the model, the reorientation of water molecules in such clusters can occur near the orientation defect. One should bear in mind that the nature of orientation defects in water and ice is very complex.²³

In the framework of the model suggested above, the observed temperature dependence of the relaxation time can be described in the following way. The increase in temperature leads, on one hand, to an increase in the probability to attain sufficient energy to break the bonds between the reorienting molecule and its neighbors (see eq 5). On the other hand, it leads to a decrease in the probability of finding a defect in the vicinity of the moving molecule (see eq 9). The interplay of these two terms in eq 11 yields the appearance of the minimum observed in the temperature dependence of the relaxation time.

The fitting results are presented in Table 2. The fitting values of the activation energies H_a and H_d are in rather quite good agreement with the energies of molecular reorientation and defect formation in ice-like water.²⁴ From the value of parameter η we can calculate the maximum possible number of defects in 1 mole of adsorbed water, about 10^{16} – 10^{17} for all the samples. This number is about 1 order of magnitude bigger than the number of defects in bulk ice.¹⁹ This can be explained by the fact that in the water absorbed in porous glasses there are more possibilities for defect formation. One can also see the correlation between the value of the energy of defect formation H_d and the number of defects on the adsorbed water structure (see Table 2). For samples with the smaller H_d the number of defects is bigger.

The investigation of the two relaxation processes described above brings us to a new understanding of the molecular dynamics of water absorbed in the porous glasses. The first relaxation process is due to single water molecule reorientation while the second relaxation process occurs as a result of the motion of ice-like structure defects. Thus, the second relaxation

process is a cooperative one. At the same time, both types of relaxation are affected by confined geometry and by the water molecule interactions with the inner porous surface.

Acknowledgment. Dr. Ya. Ryabov thanks the Valazzi-Pikovsky Fellowship Fund and Dr. V. Arkhipov thanks the Lady Davis Fellowship Trust for the financial support of their work in the Hebrew University. We also thank Dr. Ewa Rysiakiewicz-Pasek for sample preparation.

References and Notes

- (1) Gallegos, D. P.; Smith, D. M.; Brinker, C. J. *J. Colloid Interface Sci.* **1988**, *124*, 186.
- (2) Allen, S. G.; Stephenson, P. C. L.; Strange, J. H. *J. Chem. Phys.* **1997**, *106*, 7802.
- (3) Rysiakiewicz-Pasek, E.; Marczuk, K. *J. Porous Mater.* **1996**, *3*, 17.
- (4) Agamalian, M.; Drake, J. M.; Sinha, S. K.; Axe, J. D. *Phys. Rev. E* **1997**, *55*, 3021.
- (5) Hirama, Y.; Takahashi, T.; Hino, M.; Sato, T. *J. Colloid Interface Sci.* **1996**, *184*, 349.
- (6) Pissis, P.; Laudat, J.; Daoukaki, D.; Kyritsis, A. *J. Non-Cryst. Solids* **1994**, *171*, 201.
- (7) Gutina, A.; Axelrod, E.; Puzenko, A.; Rysiakiewicz-Pasek, E.; Kozlovich, N.; Feldman, Yu. *J. Non-Cryst. Solids* **1998**, *235–237*, 302.
- (8) Puzenko, A.; Kozlovich, N.; Gutina, A.; Feldman, Yu. *Phys. Rev. B* **1999**, *60*, 14348.
- (9) Roizin, Ya. O.; Alexeev-Porov, A.; Geveliyuk, S. A.; Savin, D. P.; Mugenski, E.; Sokolska, I.; Rysiakiewicz-Pasek, E.; Marczuk, K. *Phys. Chem. Glasses* **1996**, *37*, 196.
- (10) Schaumburg, G. *Dielectrics Newsletter*, Issue, November **1997**.
- (11) Pissis, P.; Anagnostopoulou-Konsta, A.; Apekis, L.; Daoukaki-Diamanti, D.; Christodoulides, C. *J. Non-Cryst. Solids* **1991**, *131–133*, 1174.
- (12) Chan, R. K.; Davidson, D. W.; Whalley, E. *J. Chem. Phys.* **1965**, *43*, 2376.
- (13) Jonscher, A. K. *Dielectric Relaxation in Solids*; Chelsea Dielectric Press: London, 1983.
- (14) Jonscher, A. K. *Universal Relaxation Law*, Chelsea Dielectric Press: London, 1996.
- (15) Shinyashiki, N.; Yagihara, S.; Arita, I.; Mashimo, S. *J. Phys. Chem. B* **1998**, *102*, 3249.
- (16) Böttcher, C. J. F.; Bordewijk, P. *Theory of Electric Polarization*, 2nd ed.; Elsevier Science: Amsterdam, 1992.
- (17) Hasted, J. B. *Aqueous Dielectric*; William Clowes & Sons Limited: London, 1973.
- (18) Fröhlich, H. *Theory of Dielectrics*; The Clarendon Press: Oxford, 1958.
- (19) Eisenberg, D.; Kauzmann, W. *The Structure and Properties of Water*; The Clarendon Press: Oxford, 1969.
- (20) Macedo, P. B.; Litovitz, T. A. *J. Chem. Phys.* **1965**, *42*, 245.
- (21) Glasstone, S. N.; Laidler, K.; Eyring, H. *The Theory of Rate Process*; McGraw-Hill Book Company Inc.: New York, 1941.
- (22) Turnbull, D.; Morrel, H. C. *J. Chem. Phys.* **1961**, *34*, 120.
- (23) Podeszwa, R.; Buch, V. *Phys. Rev. Lett.* **1999**, *83*, 4570.
- (24) Stillinger, F. H. *Low-Frequency Dielectric Properties of Liquid and Solid Water // The Liquid State of Matter: Fluids, Simple and Complex*; North-Holland: Amsterdam, 1982.